AD

Technical Report ARWSB-TR-16013

MODELING NON-LINEAR MATERIAL PROPERTIES IN COMPOSITE MATERIALS

Michael F. Macri
Andrew G. Littlefield

June 2016

U.S. ARMY ARMAMENT RESEARCH, DEVELOPMENT AND ENGINEERING CENTER
Weapons and Software Engineering Center
U.S. Army Benét Laboratories

The views, opinions, and/or findings contained in this report are those of the author(s) and should not be construed as an official Department of the Army position, policy, or decision, unless so designated by other documentation.

The citation in this report of the names of commercial firms or commercially available products or services does not constitute official endorsement by or approval of the U.S. Government.

Destroy this report when no longer needed by any method that will prevent disclosure of its contents or reconstruction of the document. Do not return to the originator.

REPORT DOCUMENTATION PAGE

Form Approved
OMB No. 0704-0188

1. REPORT DATE *(DD-MM-YYYY)*	2. REPORT TYPE	3. DATES COVERED *(From - To)*
June 2016	Technical	

4. TITLE AND SUBTITLE
MODELING NON-LINEAR MATERIAL PROPERTIES IN COMPOSITE MATERIALS

5a. CONTRACT NUMBER

5b. GRANT NUMBER

5c. PROGRAM ELEMENT NUMBER

6. AUTHOR(S)
Michael F. Macri
Andrew G. Littlefield

5d. PROJECT NUMBER

5e. TASK NUMBER

5f. WORK UNIT NUMBER

7. PERFORMING ORGANIZATION NAME(S) AND ADDRESS(ES)
U.S. Army ARDEC
Benet Laboratories, RDAR-WSB
Watervliet, NY 12189-4000

8. PERFORMING ORGANIZATION REPORT NUMBER
ARWSB-TR-16013

9. SPONSORING/MONITORING AGENCY NAME(S) AND ADDRESS(ES)

10. SPONSOR/MONITOR'S ACRONYM(S)

11. SPONSORING/MONITORING AGENCY REPORT NUMBER

12. DISTRIBUTION AVAILABILITY STATEMENT
Approved for public release; distribution is unlimited.

13. SUPPLEMENTARY NOTES

14. ABSTRACT
Fielded and future military systems are increasingly incorporating composite materials into their design. Many of these systems subject the composites to environmental conditions that can cause variations of the mechanical properties on the global scale due to phenomena on the micro-structure. Do to the nature of these problems, one cannot assume a homogenized set of material properties in critical regions, where increased accuracy is needed to capture the complex stress field. The focus of this presentation is the incorporation of non-linear material properties into the simulation. To capture the effects of the microstructure from these composites more effectively, the multi-scale enriched partition of unity method is modified to incorporate the non-linear response from the micro-scale.

15. SUBJECT TERMS
Composite Materials; Non-Linear Material Properties; Homogenization; Multiscale Enrichment Technique; Microstructure; Thermal Strain

16. SECURITY CLASSIFICATION OF:			17. LIMITATION OF ABSTRACT	18. NUMBER OF PAGES	19a. NAME OF RESPONSIBLE PERSON
a. REPORT	b. ABSTRACT	c. THIS PAGE			Mike Macri
U	U	U	U	19	19b. TELEPONE NUMBER (*Include area code*) (518) 266-5158

INSTRUCTIONS FOR COMPLETING SF 298

1. REPORT DATE. Full publication date, including day, month, if available. Must cite at lest the year and be Year 2000 compliant, e.g., 30-06-1998; xx-08-1998; xx-xx-1998.

2. REPORT TYPE. State the type of report, such as final, technical, interim, memorandum, master's thesis, progress, quarterly, research, special, group study, etc.

3. DATES COVERED. Indicate the time during which the work was performed and the report was written, e.g., Jun 1997 - Jun 1998; 1-10 Jun 1996; May - Nov 1998; Nov 1998.

4. TITLE. Enter title and subtitle with volume number and part number, if applicable. On classified documents, enter the title classification in parentheses.

5a. CONTRACT NUMBER. Enter all contract numbers as they appear in the report, e.g. F33615-86-C-5169.

5b. GRANT NUMBER. Enter all grant numbers as they appear in the report, e.g. 1F665702D1257.

5c. PROGRAM ELEMENT NUMBER. Enter all program element numbers as they appear in the report, e.g. AFOSR-82-1234.

5d. PROJECT NUMBER. Enter al project numbers as they appear in the report, e.g. 1F665702D1257; ILIR.

5e. TASK NUMBER. Enter all task numbers as they appear in the report, e.g. 05; RF0330201; T4112.

5f. WORK UNIT NUMBER. Enter all work unit numbers as they appear in the report, e.g. 001; AFAPL30480105.

6. AUTHOR(S). Enter name(s) of person(s) responsible for writing the report, performing the research, or credited with the content of the report. The form of entry is the last name, first name, middle initial, and additional qualifiers separated by commas, e.g. Smith, Richard, Jr.

7. PERFORMING ORGANIZATION NAME(S) AND ADDRESS(ES). Self-explanatory.

8. PERFORMING ORGANIZATION REPORT NUMBER. Enter all unique alphanumeric report numbers assigned by the performing organization, e.g. BRL-1234; AFWL-TR-85-4017-Vol-21-PT-2.

9. SPONSORING/MONITORS AGENCY NAME(S) AND ADDRESS(ES). Enter the name and address of the organization(s) financially responsible for and monitoring the work.

10. SPONSOR/MONITOR'S ACRONYM(S). Enter, if available, e.g. BRL, ARDEC, NADC.

11. SPONSOR/MONITOR'S REPORT NUMBER(S). Enter report number as assigned by the sponsoring/ monitoring agency, if available, e.g. BRL-TR-829; -215.

12. DISTRIBUTION/AVAILABILITY STATEMENT. Use agency-mandated availability statements to indicate the public availability or distribution limitations of the report. If additional limitations/restrictions or special markings are indicated, follow agency authorization procedures, e.g. RD/FRD, PROPIN, ITAR, etc. Include copyright information.

13. SUPPLEMENTARY NOTES. Enter information not included elsewhere such as: prepared in cooperation with; translation of; report supersedes; old edition number, etc.

14. ABSTRACT. A brief (approximately 200 words) factual summary of the most significant information.

15. SUBJECT TERMS. Key words or phrases identifying major concepts in the report.

16. SECURITY CLASSIFICATION. Enter security classification in accordance with security classification regulations, e.g. U, C, S, etc. If this form contains classified information, stamp classification level on the top and bottom of this page.

17. LIMITATION OF ABSTRACT. This block must be completed to assign a distribution limitation to the abstract. Enter UU (Unclassified Unlimited) or SAR (Same as Report). An entry in this block is necessary if the abstract is to be limited.

ABSTRACT

Fielded and future military systems are increasingly incorporating composite materials into their design. Many of these systems subject the composites to environmental conditions that can cause variations of the mechanical properties on the global scale due to phenomena on the micro-structure. Do to the nature of these problems, one cannot assume a homogenized set of material properties in critical regions, where increased accuracy is needed to capture the complex stress field. The focus of this presentation is the incorporation of non-linear material properties into the simulation. To capture the effects of the microstructure from these composites more effectively, the multi-scale enriched partition of unity method is modified to incorporate the non-linear response from the micro-scale.

TABLE OF CONTENTS

LIST OF FIGURES

LIST OF TABLES

1. INTRODUCTION

Modeling composite materials poses a significant computational challenge, requiring the capability to implement the material response accurately and efficiently optimizing the computational cost. To accurately simulate composite material, the orthotropic effects should be incorporated by importing empirical data [1] or using assumptions within theoretical calculations. The most notable contribution to the composite material properties is the reaction from the local micro-structure especially in critical regions, such as high temperature changes. However, within these critical regions incorporating the microstructure effect has proven to be problematic. A full finite element solution traversed down to the microscopic level, taking into account the detailed micro-structural features within these areas, is currently computationally infeasible. Hence a robust and reliable multiscale computational technique is necessary to account the microstructure phenomena.

Though empirical data can be used to approximate the material properties for an ideal non-damaged specimen, performing experimentation on damaged composites and extracting a correlation between micro-structure effects to material properties can be extremely difficult. As an alternative, material properties from a composite material can be extracted using a numerical approximation method, referred to as the homogenization method [2]. This method uses asymptotic expansions of field variables about macroscopic values and provides overall effective properties as well as microscopic stress and strain values for a local point on the global model. The primary limitation with this method is that it assumes uniformity of the macroscopic fields within each representative volume element (RVE). Hence, this method breaks down in critical regions of high gradients. To resolve the limitation of the homogenization method within critical regions, several multiscale methods have been presented which are reviewed by Macri et al. in reference [3].

To overcome the drawbacks of the existing methods [3, 4] proposed a structural based enrichment method based on the principles of partition of unity which allows enrichment of the approximation space in localized sub domains using specialized functions that may be generated based on a priori information regarding asymptotic expansions of local stress fields and microstructure. One of the major advantages of the partition of unity-based enrichment strategies is that the enriched local function space may be easily varied from one node to the other.

In this presentation, we focus on the incorporation of non-linear material properties into the simulation. Most composites will be composed of materials that are temperature dependent. As the composite is heated, the simulation will constantly need to check and update the material properties. As documented in [5], this translates to updating the effective properties for the homogenization method at every time step. In [6], a similar approach is addressed for structural enrichment occurring in mechanical simulations. In this paper, we discuss how temperature dependencies are implemented for thermal simulations.

In the next section, we briefly review the homogenization and enrichment methods and how temperature dependent material properties are incorporated into the simulation. And in section 3, we demonstrate an example of the approach.

2. EXPERIMENTATION

We have divided this section into two parts. Section 2.1 reviews the concepts of the homogenization method and how non-linearity is implemented. In section 2.2 we discuss how this is implemented for structural enrichment.

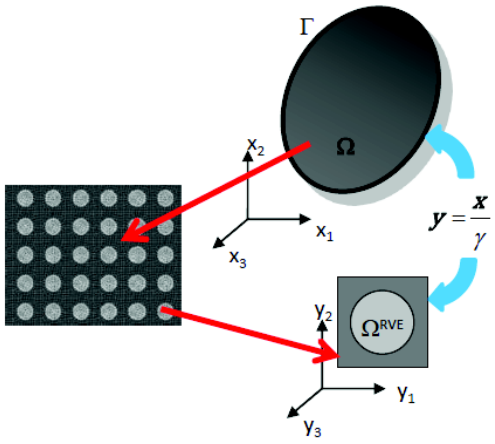

Figure 1. Multi-scale homogenization approach

2.1 Review of the Homogenization Approach

The homogenization theory [2], assumes multiple scales related by a scale factor, γ. In the case of two scales:

$$\boldsymbol{y} = \frac{\boldsymbol{x}}{\gamma} \qquad [1]$$

where ***x*** and ***y*** represent a global and microscale, respectively (see Figure 1). A function spanning the scales can be defined by

$$f^{\gamma}(x) = f\big(\boldsymbol{x}, \boldsymbol{y}(\boldsymbol{x})\big) \qquad [2]$$

Such that the microscale is dependent on the global scale. The homogenization approach assumes local-periodicity on the micro-scale. Thus, a representative volume element (RVE), as shown in Figure 1, with a side length of *Y* can be depicted as:

$$f\big(x_i, y_j\big) = f\big(x_i, y_j + kY_j\big) \qquad [3]$$

where *k* is the periodic interval. Using asymptotic expansion, we can write the field variables, such as displacement, as:

$$T^{\gamma}(\boldsymbol{x}, \boldsymbol{y}) = T^{0}(\boldsymbol{x}, \boldsymbol{y}) + \gamma T^{1}(\boldsymbol{x}, \boldsymbol{y}) + \mathcal{O}(\gamma^{2}) \qquad [4]$$

In this presentation we assume a thermo-elastic response for the system. The equations governing this thermal analysis are:

$$\left(k_{ij}T^{\gamma}_{,x_j}\right)_{,x_i} + Q - \rho c T^{\gamma}_{,t} = 0 \quad \in \Omega \tag{5a}$$

$$T^{\gamma} = T_g \qquad \in \Gamma_{\mathrm{g}} \tag{5b}$$

$$-k_{ij}T^{\gamma}_{,x_j}n_i = q \quad \in \Gamma_{\mathrm{q}} \tag{5c}$$

The $\boldsymbol{k}$ term represents thermal conductivity, Q is a heat supply per unit volume, and T_g and q are the prescribed temperatures and heat flux, respectively.

The thermal strains are calculated such that:

$$\varepsilon^{T}_{kl} = \alpha_{kl}\theta^{\gamma} \tag{6}$$

Where ϑ^{γ} is the change in temperature, defined as:

$$\theta^{\gamma} = T^{\gamma} - T_I \tag{7}$$

where T_I is the initial temperature. The change in temperature field, θ^{γ}, will be used to calculate the thermal strains. In equation [6], $\boldsymbol{\alpha}$ is the coefficient of thermal expansion tensor.

To determine the effects of the micro-structure across the domain, we substitute the asymptotic expansion of the temperature into the heat equation, [5]. Rearranging the terms gives us:

$$\begin{aligned}
&\gamma^{-2}\left[\left(k_{ij}T^{0}_{,y_j}\right)_{,y_i}\right] + \\
&\gamma^{-1}\left[\left(k_{ij}T^{0}_{,x_j}\right)_{,y_i} + \left(k_{ij}T^{0}_{,y_j}\right)_{,x_i} + \left(k_{ij}T^{1}_{,y_j}\right)_{,y_i}\right] + \\
&\gamma^{0}\left[\left(k_{ij}T^{0}_{,x_j}\right)_{,x_i} + \left(k_{ij}T^{1}_{,x_j}\right)_{,y_i} + \left(k_{ij}T^{1}_{,y_j}\right)_{,x_i} + Q - \rho c T^{0}_{,t}\right] + \mathcal{O}(\gamma) = 0
\end{aligned} \tag{8}$$

By setting each order γ^{i} term to zero, it is straightforward to derive the following

$$T^{0}(\boldsymbol{x},\boldsymbol{y}) = T^{0}(\boldsymbol{x}) \tag{9a}$$

$$\left[k_{ij}\left(I_{mj} + H^{k}_{m,y_j}\right)\right]_{,y_i} = 0 \quad \epsilon\Omega^{RVE} \tag{9b}$$

$$\left[\tilde{k}_{ij}T^{0}_{,x_j}\right]_{,x_i} + \tilde{Q} - \tilde{\rho}\tilde{c}T^{0}_{,t} = 0 \qquad \epsilon\Omega \tag{9c}$$

Equation [9a] states that T^{0} is only dependent on the global scale, $\boldsymbol{x}$. Equation [9b] is the governing equation for the microscale, where $\boldsymbol{I}$ is the identity tensor and $\boldsymbol{H^{k}(y)}$ is a Y-periodic tensor on the micro-scale relating T^{1} to the macro-scale, such that:

$$T^{1}(\boldsymbol{x},\boldsymbol{y}) = H^{k}_{m}(\boldsymbol{y})T^{0}_{,x_m}(\boldsymbol{x}) \tag{12}$$

where m is based on the dimensionality of the problem. Equation [9c] is the governing equation for the global scale. In this equation, $\widetilde{\boldsymbol{k}}$ represents the effective thermal conductivity tensor, $\tilde{\rho}$ is the effective density, $\tilde{c}$ is the effective specific heat and $\tilde{Q}$ is the effective heat supply. They are defined as:

$$\tilde{k}_{ij} = \frac{1}{V^{RVE}} \int_{\Omega^{RVE}} k_{ij} \left(I_{mj} + H^{k}_{m,y_j} \right) \partial \Omega^{RVE} \quad [13]$$

$$\tilde{\rho} = \frac{1}{V^{RVE}} \int_{\Omega^{RVE}} \rho \partial \Omega^{RVE} \quad [14]$$

$$\tilde{c} = \frac{1}{V^{RVE}} \int_{\Omega^{RVE}} c \partial \Omega^{RVE} \quad [15]$$

$$\tilde{Q} = \frac{1}{V^{RVE}} \int_{\Omega^{RVE}} Q \partial \Omega^{RVE} \quad [16]$$

For an implicit time simulations the well documented weak form of 9c can be written as

$$(\boldsymbol{M} + \Delta t \boldsymbol{K})^{t+\Delta t} \boldsymbol{a} = \Delta t \boldsymbol{F} + \boldsymbol{M}\ {}^{t}\boldsymbol{a} \quad [17]$$

$$\boldsymbol{M} = \int_{\Omega} \boldsymbol{N}^{T} \tilde{\rho} \tilde{c} \boldsymbol{N} \partial \Omega \quad [18]$$

$$\boldsymbol{K} = \int_{\Omega} \boldsymbol{B}^{T} \tilde{k} \boldsymbol{B} \partial \Omega \quad [19]$$

$$\boldsymbol{F} = \int_{\Omega} \boldsymbol{N}^{T} \tilde{Q}(t + \Delta t) \partial \Omega + \int_{\Gamma} \boldsymbol{N}^{T} \bar{q}(t + \Delta t) \partial \Gamma \quad [20]$$

where ***N*** is the finite element shape functions, ***B*** are the derivatives of ***N*** with respect to coordinates, *Δt* is the change in time and $\bar{q}$is the heat flux. The global temperature at time, *t*, is defined as:

$${}^{t}T^{0}(\boldsymbol{x}) = \boldsymbol{N}(\boldsymbol{x})\ {}^{t}\boldsymbol{a} \quad [21]$$

For simplicity, we assume problems consisting of temperature dependent thermal conductivity. Thus, equation [13] becomes:

$$\tilde{k}\left({}^{t+\Delta t}T^{\Upsilon}\right)_{ij} = \frac{1}{V^{RVE}} \int_{\Omega^{RVE}} k\left({}^{t+\Delta t}T^{\Upsilon}\right)_{ij} \left(I_{mj} + H^{k}_{m,y_j} \right) \partial \Omega^{RVE} \quad [22]$$

For linear temperature independent simulations, $\tilde{k}$ is calculated once at the beginning of the simulation. However, since it is assumed that ${}^{t+\Delta t}T^{\Upsilon}$ will vary across the model and with each time step, unlike linear simulations, $\tilde{k}$ will need to be calculated at each integration point within the model, for each time step.

For an implicit simulation we calculate $\tilde{k}$ at time step t+Δt. Thus, equations [17] and [19], can be rewritten, respectfully, as:

$$\left(\boldsymbol{M} + \Delta t\, {}^{\boldsymbol{t+\Delta t}}\boldsymbol{K}\right)^{t+\Delta t} \boldsymbol{a} = \Delta t \boldsymbol{F} + \boldsymbol{M}\ {}^{t}\boldsymbol{a} \quad [23]$$

$${}^{\boldsymbol{t+\Delta t}}\boldsymbol{K} = \int_{\Omega} \boldsymbol{B}^{T}\, {}^{t+\Delta t}\tilde{k} \boldsymbol{B} \partial \Omega \quad [24]$$

Because of ***K***'s dependency of time, equation [23] requires a non-linear approach at each time step to solve for $^{t+\Delta t}\mathbf{a}$. Using Tayler series expansion of [23] about $^{t+\Delta t}\mathbf{a}$ and the Newton-Raphson method we can write the iterative equations as:

$$\boldsymbol{J}^{(j-1)}\boldsymbol{\Delta a}^{j} = \Delta t\boldsymbol{F} + \boldsymbol{M}\ {}^{t}\boldsymbol{a} - \left(\boldsymbol{M} + \Delta t^{\boldsymbol{t+\Delta t}}\boldsymbol{K}^{(j-1)}\right)^{t+\Delta t}\boldsymbol{a}^{(j-1)} \quad [25]$$

$$^{t+\Delta t}\boldsymbol{a}^{(j)} = \boldsymbol{\Delta a}^{j} + {}^{t+\Delta t}\boldsymbol{a}^{(j-1)} \quad [26]$$

where $\boldsymbol{J}^{(j-1)}$ is the derivative of [23] with respect to $^{t+\Delta t}\mathbf{a}$ that is dependent on the relationship between the thermal conductivity and temperature.

Thus the process at each time step is outlined as:

1. *Set* $^{t+\Delta t}\boldsymbol{\alpha}^{0} = {}^{t}\boldsymbol{\alpha}$ *for all nodes not on an essential boundary*
2. *Set j=1*
3. *While (not-converged)*
    a. Calculate $\tilde{k}\left({}^{t+\Delta t}T^{(j-1)}\right)$ *for each integration point within the model*
    b. *Setup* $\boldsymbol{J}^{(j-1)}\boldsymbol{\Delta a}^{j} = \Delta t\boldsymbol{F} + \boldsymbol{M}\ {}^{t}\boldsymbol{a} - \left(\boldsymbol{M} + \Delta t^{\boldsymbol{t+\Delta t}}\boldsymbol{K}^{(j-1)}\right)^{t+\Delta t}\boldsymbol{a}^{(j-1)}$
    c. *Solve for* $\boldsymbol{\Delta\alpha}^{j}$
    d. *Set* $^{t+\Delta t}\boldsymbol{\alpha}^{(j)} = {}^{t+\Delta t}\boldsymbol{\alpha}^{(j-1)} + \boldsymbol{\Delta\alpha}^{j}$
    e. Set j=j+1
    f. If $\left\|\boldsymbol{\Delta a}^{j}\right\|_{2} < tolerence$*, set status to converged*
4. *End while loop*

For the example in section 3, we will be examining the thermal strains generated from the simulation. In reference [7] we define the effective coefficient of thermal expansion as:

$$\tilde{\alpha}_{kl} = \frac{1}{V^{RVE}}\int_{\Omega^{RVE}} C_{ijkl}\left(H^{\theta}_{k,y_l} - \alpha_{kl}\right)\partial\Omega^{RVE} \quad [27]$$

2.2 Implementation of Damaged Microstructure

Within this section we review the partition of unity paradigm and how it is implemented, followed by the derivation of the enrichment functions.

2.2.1 Interpolation Functions

The partition of unity paradigm requires that the sum of all functions at a given point in a domain is equal to one, such that

$$\sum_{i=1}^{N}\varphi_{I}^{0}(\boldsymbol{x}) = 1 \quad [28]$$

In the above equation, φ_{I}^{0} is the I^{th} partition of unity function and *N* is the total number of partition of unity functions within the domain, *Ω*. Thus, the sum of all the functions at a given point, ***x***, within *Ω* will equal 1.

Based on this concept we define the global approximation space, for a method using interpolation functions, as:

$$V^{h,p} = \sum_{I=1}^{N} \varphi_I^0 V_I^{h,p} \subset H^1(\Omega) \quad [29]$$

where the superscripts *h* and *p* are the size of the element and the polynomial order, respectively. H^1 is the first order Hilbert space and $V_I^{h,p}$ is the local approximation space at *I*, defined as:

$$V_I^{h,p} = span_{m\in\zeta}\{p_m(\boldsymbol{x})\} \subset H^1(\bar{B}_I \cap \Omega) \quad [30]$$

In equation [17], ζ is an index set, $\bar{B}_I$ is the support for node *I* and $p_m(\boldsymbol{x})$ is composed of polynomials or other functions. From the above equations we can write any function $v^{h,p}$ within the global approximation space as:

$$v^{h,p}(x) = \sum_{I=1}^{N} \sum_{m\in\zeta} h_{Im}(\boldsymbol{x}) a_{Im}\,, \qquad v^{h,p} \in V^{h,p} \quad [31]$$

where

$$h_{Im}(\boldsymbol{x}) = \varphi_I^0(\boldsymbol{x}) p_m(\boldsymbol{x}) \quad [32]$$

is the interpolation function at node *I*, corresponding to the m^{th} degree of freedom, and a_{Im} is the associated degree of freedom.

For FEA, the standard shape function, N_I, which can be referenced in numerous sources, satisfies the partition of unity criteria for φ_I^0. For a typical finite element analysis, correlating the definition of a finite element shape function to the interpolation function in equation [32], requires that $p_m = span\{1\}$. Reference [7] discusses other partition of unity functions and basis that can be implemented.

2.2.2 Enrichment Functions

In the previous section, we defined a function in the global approximation space as the sum of the partition of unity functions multiplied by a group of basis functions and associated degrees of freedom. Focusing on the basis functions, $p_n(\boldsymbol{x})$, we state that if an arbitrary function is included in the local basis of all nodes within the domain and assuming $\alpha_{Im} = \delta_{mn}\ \forall I$ then

$$\sum_{I=1}^{N} \sum_{m\epsilon\zeta} \phi_I^0(\boldsymbol{x}) p_m(\boldsymbol{x}) a_{Im} = p_n(x) \left(\sum_{I=1}^{N} \phi_I^0(\boldsymbol{x}) \right) = p_n(\boldsymbol{x}) \quad [33]$$

Equation [33] demonstrates that it is possible to exactly reproduce a function over the entire domain. This fundamental concept enables the consistency of the interpolation functions to be adjusted based on the population of the basis functions. Thus, we can expend the basis function to include relevant functions to enforce a known displacement field.

To derive the structural based enrichment function, we examine the asymptotic expansion of the temperature field. Substituting equation [12] into [4] gives us:

$$T^{\gamma}(\boldsymbol{x}, \boldsymbol{y}) = T^0(\boldsymbol{x}) + \gamma H_n^k(\boldsymbol{y}) T_{,x_n}^0(\boldsymbol{x}) \quad [34]$$

For a single-scale problem, we define the displacement field, assuming linear consistency in 2D, as

$$T^0(\boldsymbol{x}) = \sum_{I=1}^{N} \sum_{m\epsilon\zeta} \phi_I^0(\boldsymbol{x}) p_m(\boldsymbol{x}) a_{Im} \quad [35]$$

where $\varphi_I^0$and p_m are N_I and $p_m = span\{1\}$.

To perform a multi-scale analysis, we need to incorporate the second term on the right hand side of equations [34]. We focus on the Y-periodic tensors. Details of the derivation are given in [6]. The resulting basis functions for a two-dimensional thermal problem are given as:

$$p_m = span\{1, H_1^k(\boldsymbol{y}(\boldsymbol{x})), H_2^k(\boldsymbol{y}(\boldsymbol{x}))\} \quad [36]$$

Thus using equation [32], we can define T^γ as:

$$T^\gamma(\boldsymbol{x}) = h_{Im}(x) a_{Im} \quad [37]$$

where $\varphi_I^0$is defined as N_I and p_m is defined by equation [36].

2.2.3 Implementation the Multiscale Enrichment Technique

The approach to implementing structural based enrichment varies depending on the governing method. In this presentation we will focus in the FEA approach. Reference [4] gives complete details on the implementation of the multiscale enrichment into FEA. In this section we will briefly review how the algorithm is applied.

The analysis is based on a homogenization-like integration (HLI) scheme [4]. The solution requires the enrichment functions and the material properties, which are only known on the micro-scale, ***y***. To implement this technique and resolve the aforementioned issue, integration will be performed on an RVE transformed to the macro-scale, ***x***, coordinate system. The HLI scheme, shown in Figure 2, is based on the assumption that there is a significant deference between the two scales and that the Gauss points used for FEA are sparse with respect to the size of the RVE. In this approach, an RVE is centered on each Gauss point within macro-scale problem. An integrand, *I*, on the macro-scale is replaced with the following

$$I = \int_\Omega J\upsilon \, \partial\Omega = \sum_{i=1}^{n_{guass}} W_i J_i \upsilon(\boldsymbol{x}_i^{GP}) = \sum_{i=1}^{n_{guass}} W_i J_i \frac{1}{V^{RVE}} \int_{\bar{\Omega}_i^{\mathrm{RVE}}} \upsilon(\boldsymbol{x}) \, \partial\bar{\Omega}_i^{\mathrm{RVE}} \quad [38]$$

Where υ is an arbitrary function, $\boldsymbol{x}_i^{GP}$ is the *i*th Gauss point, $\bar{\Omega}_i^{RVE}$ is the domain of an RVE centered on the *i*th Gauss point, *J* is the Jacobian and W_i is a weight associated with the *i*th Gauss point. Reference [4] has demonstrated that the accuracy of HLI improves with decreasing size of the RVE. Thus, this implementation works well when the difference in scales is significant. However, as the scales become closer and the therefore the volume of the RVE increases, equation [34] will develop convergence errors.

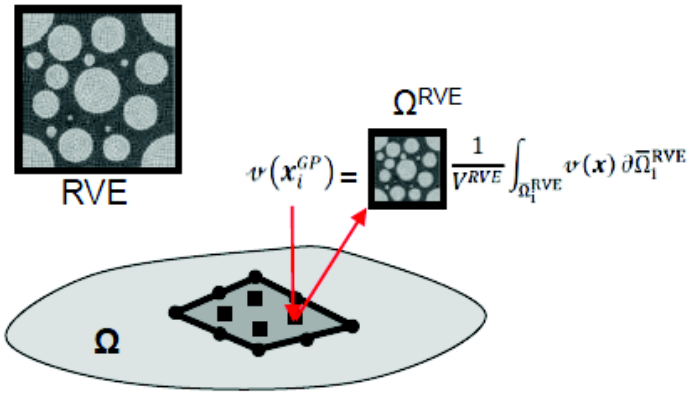

Figure 2. Implementation of multiscale enrichment into FEA

2.2.4 Implementation of the Multiscale Enrichment Technique for Non-Linear Simulation

For an implicit time simulations using structural enrichment techniques, the weak form of the governing equation is setup similar to the homogenization approach

$$(\boldsymbol{M} + \Delta t \boldsymbol{K})^{t+\Delta t}\boldsymbol{a} = \Delta t \boldsymbol{F} + \boldsymbol{M}\ {}^{t}\boldsymbol{a} \quad [39]$$

$$\boldsymbol{M} = \int_{\Omega} \boldsymbol{h}^{T} \rho c \boldsymbol{h} \partial\Omega \quad [40]$$

$$\boldsymbol{K} = \int_{\Omega} \tilde{\boldsymbol{B}}^{T} k \tilde{\boldsymbol{B}} \partial\Omega \quad [41]$$

$$\boldsymbol{F} = \int_{\Omega} \boldsymbol{h}^{T} Q(t+\Delta t) \partial\Omega + \int_{\Gamma} \boldsymbol{h}^{T} \bar{q}(t+\Delta t) \partial\Gamma \quad [42]$$

where $\boldsymbol{h}$ is defined in [37] and $\tilde{B}$ is the derivatives of $\boldsymbol{h}$ with respect to coordinates. The global temperature at time, t, is defined as:

$${}^{t}T^{0}(\boldsymbol{x}) = \boldsymbol{h}(\boldsymbol{x})\ {}^{t}\boldsymbol{a} \quad [43]$$

For problems consisting of temperature dependent thermal conductivity, equations [39] and [41] can be rewritten, respectfully, as:

$$\left(\boldsymbol{M} + \Delta t^{\boldsymbol{t+\Delta t}}\boldsymbol{K}\right)^{t+\Delta t}\boldsymbol{a} = \Delta t \boldsymbol{F} + \boldsymbol{M}\ {}^{t}\boldsymbol{a} \quad [44]$$

$${}^{\boldsymbol{t+\Delta t}}\boldsymbol{K} = \int_{\Omega} \boldsymbol{B}^{T}\, {}^{t+\Delta t}k \boldsymbol{B} \partial\Omega \quad [45]$$

Because the basis of $\boldsymbol{h}$ is composed of H_m^K, we need to examine equation [9b], which will now be adjusted to account for the temperature dependency.

$$\left[k\left({}^{t+\Delta t}T^{\Upsilon}\right)_{ij}\left(I_{mj} + H^{k}_{m,y_j}\right)\right]_{,y_i} = 0 \quad \epsilon\Omega^{RVE} \quad [46]$$

Since it is assumed that ${}^{t+\Delta t}T^{\Upsilon}$ will vary across the model and with each time step, H_m^K will need to be calculated at each integration point within the model, for each time step.

Using Tayler series expansion of [44] about ${}^{t+\Delta t}\mathbf{a}$ and the Newton-Raphson method we can write the iterative equations as:

$$\boldsymbol{J}^{(j-1)}\boldsymbol{\Delta a}^{j} = \Delta t\boldsymbol{F}^{(j-1)} + \boldsymbol{M}^{(j-1)}\ {}^{t}\boldsymbol{a} - \left(\boldsymbol{M}^{(j-1)} + \Delta t^{\boldsymbol{t+\Delta t}}\boldsymbol{K}^{(j-1)}\right)^{t+\Delta t}\boldsymbol{a}^{(j-1)} \qquad [47]$$

Where $\boldsymbol{J}^{(j-1)}$ is the derivative of [44] with respect to ${}^{t+\Delta t}\mathbf{a}$ that is dependent on the relationship between the thermal conductivity and temperature.

Thus the process at each time step is outlined as:

1. *Set* ${}^{t+\Delta t}\boldsymbol{\alpha}^{0} = {}^{t}\boldsymbol{\alpha}$ *for all nodes not on an essential boundary*
2. *Set j=1*
3. *While (not-converged)*
    a. Calculate H_m^K *for each integration point within the model*
    b. Setup equation [47]
    c. Solve for $\boldsymbol{\Delta\alpha}^{j}$
    d. *Set* ${}^{t+\Delta t}\boldsymbol{\alpha}^{(j)} = {}^{t+\Delta t}\boldsymbol{\alpha}^{(j-1)} + \boldsymbol{\Delta\alpha}^{j}$
    e. Set j=j+1
    f. If $\left\|\boldsymbol{\Delta a}^{j}\right\|_2 < tolerence$*, set status to converged*
4. *End while loop*

3. RESULTS

We examined a two-dimensional cross section of a composite wafer with a hole, depicted in Figure 3. The dynamic simulation was modeled assuming an implicit time step. A temperature change on the hole was implemented to induce thermal stress. In this example, we examine the upper right quadrant of the cross sectional area. The composite is composed of Al_2O_3 fibers, all orientated perpendicular to the cross section, within an Aluminum matrix. The material properties are given in Tables 1 through 3. The RVEs, were modeled using 150 quadratic 1st order elements. The boundary conditions on the global model were a heat source that linearly increased on the surface of the hole from $22℃$ to $400℃$ over a second. The course model was simulated with 102 linear triangular elements. The results were compared to a fine mesh, Figure 3a, composed of $5.2\text{x}10^6$ quadratic 1st order elements modeled down to the micro-scale.

The results for the temperature fields across the model are shown in Figures 4. The results show a similar temperature field after 1s for all three cases. The focus of our examination is the thermal strain, $\boldsymbol{\varepsilon}^{\boldsymbol{T}}$, occurring on the micro-structure. Figures 5-7 show the thermal strains on the RVEs at five locations within the model and visually show similar results for all three cases. However, if we examine the error in the solutions in tables 4 and 5, we see that structural enrichment is improving the simulation, ranging from an error reduction of 0.5% to 12%.

Table 1. Material properties of RVE

Material	α (ºC^{-1})	ρ (tonne/mm^3)	c (mJ/tonne ºC)
Aluminum	2.2x10^{-5}	2.7x10^{-9}	8.98x10^8
Al_2O_3	4.9 x10^{-5}	1.15x10^{-9}	1.7x10^9

Table 2. Thermal conductivity for aluminum

ºC	k (mW/(mmºC))
22	237
77	240
126	236
227	236
327	231
527	218

Table 3. Thermal conductivity for Al_2O_3

ºC	k (mW/(mmºC))
92	0.12
204	0.13
315	0.14
404	0.15

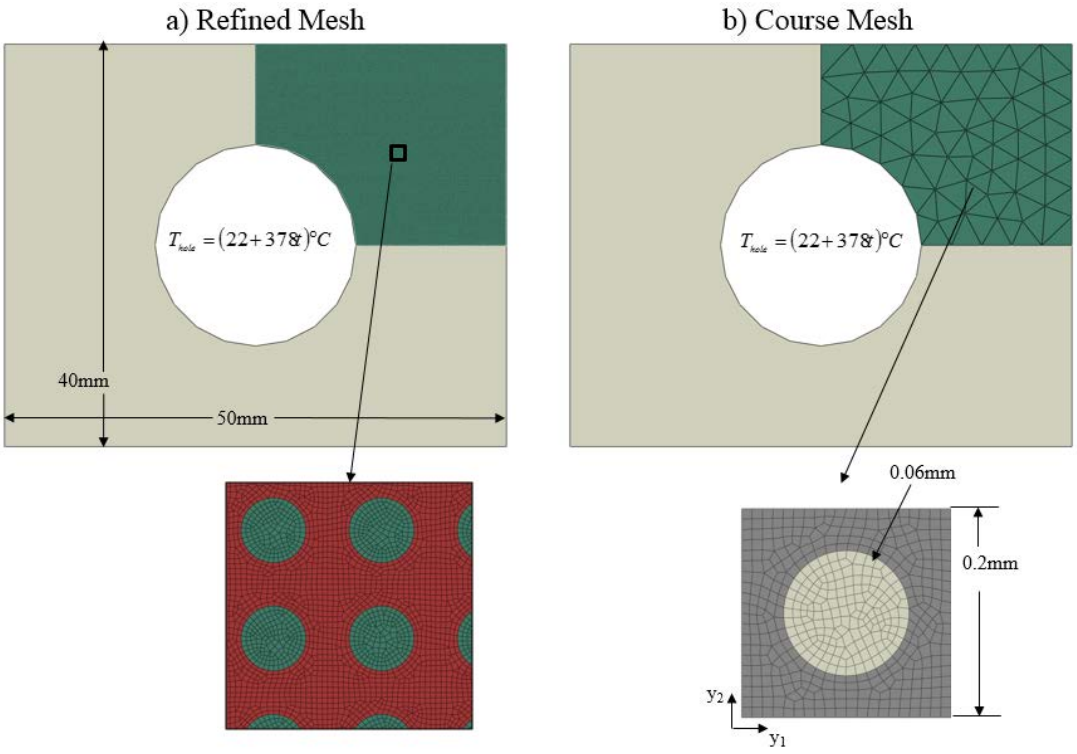

Figure 3. Composite sample

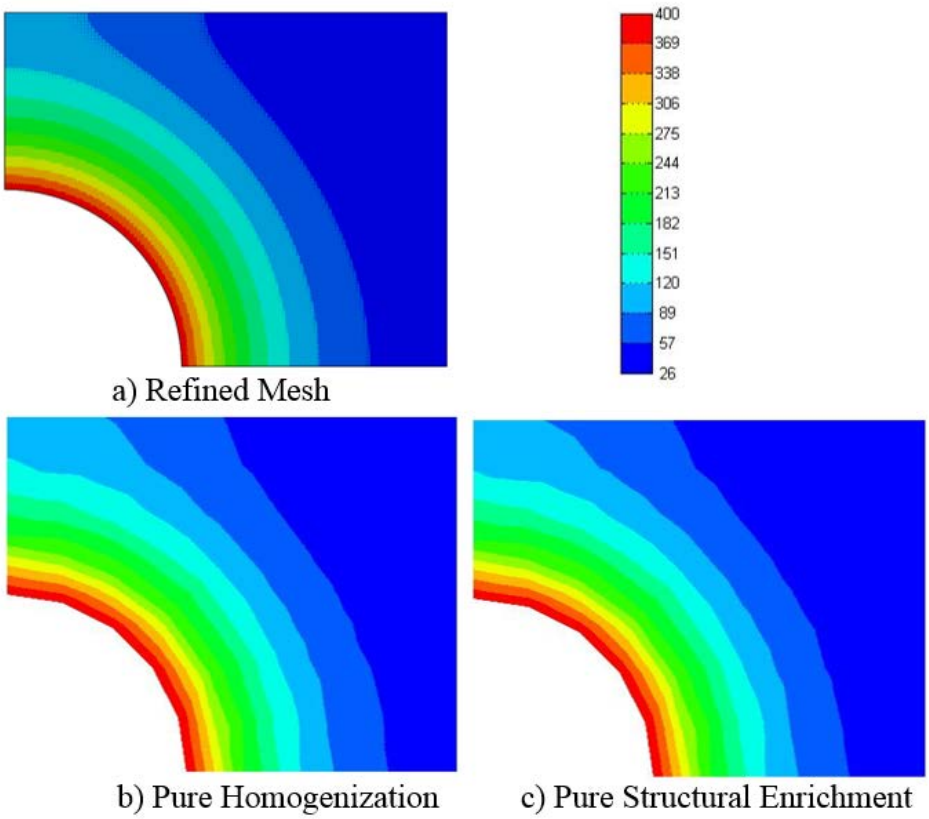

Figure 4: Temperature fields after 1s

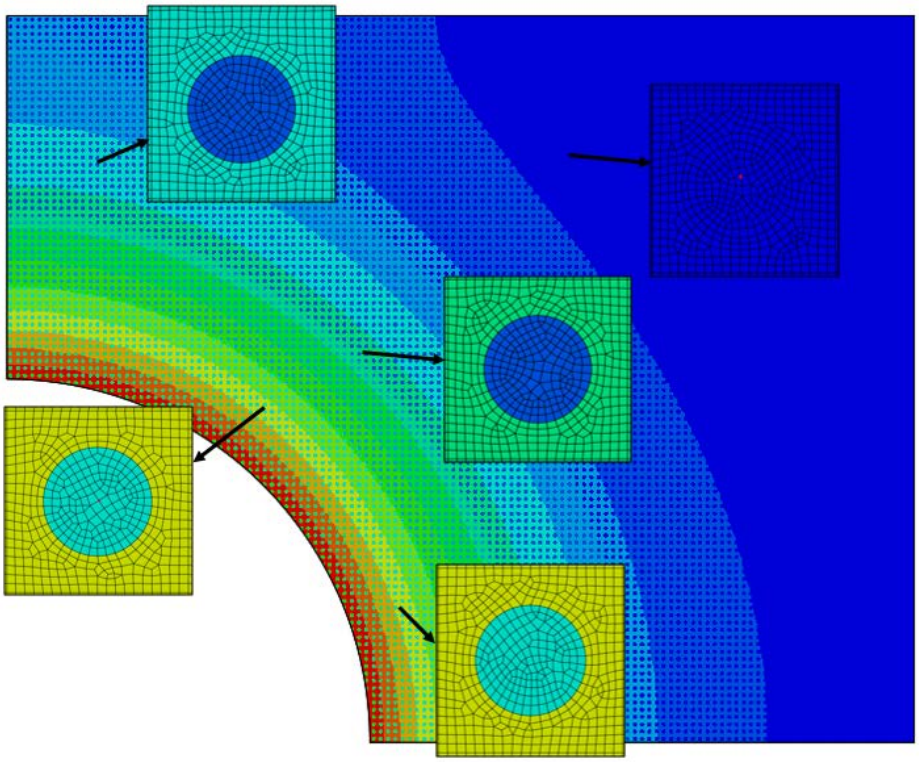

Figure 5: Thermal strains on refined mesh after 1s

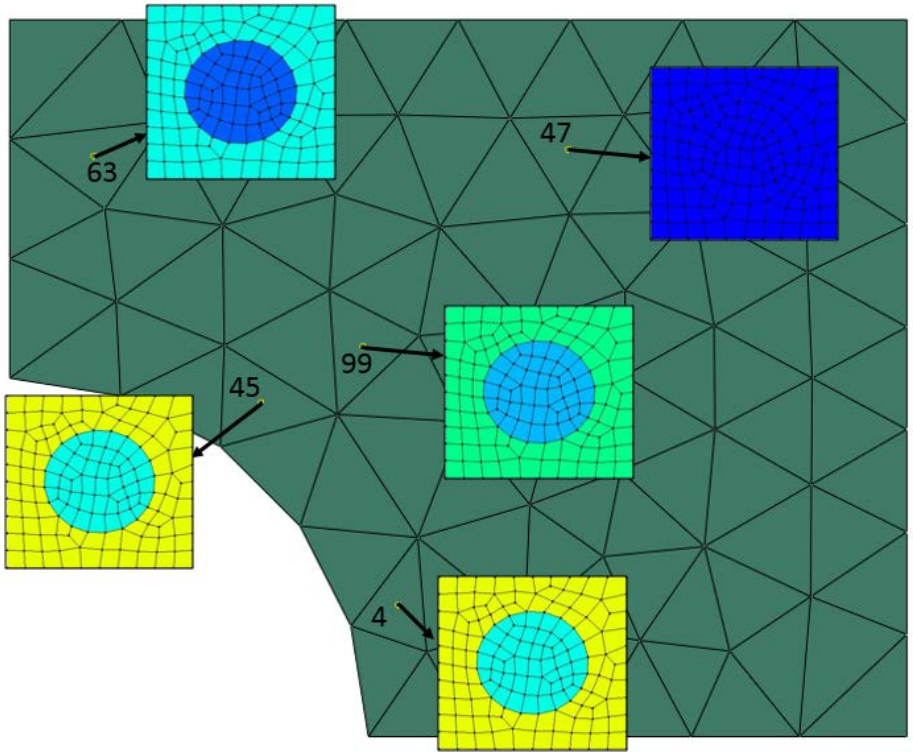

Figure 6: Thermal strains for homogenization after 1s

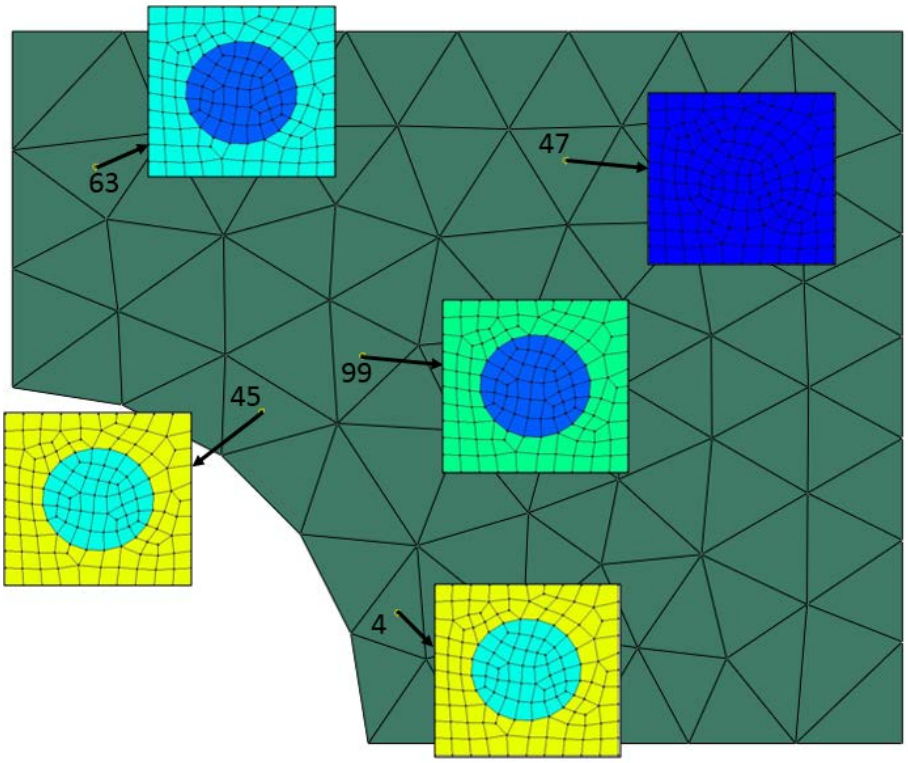

Figure 7: Thermal strains for structural enrichment after 1s

Table 4: Error in thermal strains at gauss points of course mesh for homogenization

Element #	Matrix (Al)		Fiber (Al2O3)	
	Avg ε^T (mm/mm)	Relative Error (%)	Avg ε^T (mm/mm)	Relative Error (%)
4	1.381×10^{-2}	3.7	6.198×10^{-3}	5.09
45	1.325×10^{-2}	3.25	5.951×10^{-3}	4.81
63	5.454×10^{-3}	3.97	2.449×10^{-3}	6.49
99	7.128×10^{-3}	4.01	3.200×10^{-3}	5.92
47	1.327×10^{-3}	10.01	5.957×10^{-4}	13.5

Table 5: Error in thermal strains at gauss points of course mesh for structural enrichment

Element #	Matrix (Al)		Fiber (Al2O3)	
	Avg ε^T (mm/mm)	Relative Error (%)	Avg ε^T (mm/mm)	Relative Error (%)
4	$1.377x10^{-2}$	3.48	$6.184x10^{-3}$	4.87
45	$1.320x10^{-2}$	2.87	$5.927x10^{-3}$	4.43
63	$5.264x10^{-3}$	0.5	$2.363x10^{-3}$	3.11
99	$6986.x10^{-3}$	2.05	$3.136x10^{-3}$	4.01
47	$1.149x10^{-3}$	3.98	$5.159x10^{-4}$	0.12

4. CONCLUSIONS

In this paper, we have adapted the structural enrichment meth to incorporate non-linear material properties within the composite. Using structural enrichment requires that the material and enriched shape functions be updated for all elements at each time step. The results show an improvement in the thermal strain calculations, for the example shown, when using the structural enrichment techniques over pure homogenization, ranging from 0.5% to 12%.

5. REFERENCES

1. Nemat-Nasser, S & Hori, M. Micromechanics: Overall Properties of Heterogeneous Materials, North-Holland, London, 1993.

2. Bakhalov, N. & Panasenko, G. *Homogenization: Averaging process in periodic media*. Dordrecht: Kluer: Academic Publishers, 1989.

3. Macri, M. & De, S. “An octree partition of unity method (OctPUM) with enrichments for multiscale modeling of heterogeneous media.” *Computers & Structures* 86 (2008): 780–795.

4. Fish, J. & Yuan, Z. “Multiscale enrichment based on partition of unity.” *International Journal for Numerical Methods in Engineering* 24 (2005): 1341–1359.

5. Fish J. Practical Multiscaling. West Sussex, UK: John Wiley & Sons, 2014

6. Fish, J. & Yuan, Z. “Multiscale Enrichment based on Partition of Unity for Nonperiodic Fields and Nonlinear Problems.” *Computational Mechanics* 40 (2007): 249-259.

7. Macri, M. & Littlefield A. “Enrichment Based Multi-scale Modeling of Composite Materials undergoing Thermo-Stress”, *International Journal for Numerical Methods in Engineering* 93 (2013): 1147-1169.